J Supercond Nov Magn (2015) 28:379–382
DOI 10.1007/s10948-014-2723-9

ORIGINAL PAPER

# Substrate Influence on Dendritic Flux Instability in YBCO Thin Films

**E. Baruch-El · M. Baziljevich · T. H. Johansen · Y. Yeshurun**

Received: 9 June 2014 / Accepted: 18 August 2014 / Published online: 3 September 2014

**Abstract** We have investigated the effect of substrate thermal conductivity on dendritic flux formation in thin superconducting $YBa_2Cu_3O_{7-x}$ films grown on yttrium-stabilized zirconia, $SrTiO_3$, MgO, and sapphire, exploiting a recently developed ultra-fast magneto-optical imaging system and its ultra-fast field ramp (3 kT/s). Dendritic flux formation triggered solely by rapid ramping of the external field is reported for the first time in YBCO on yttrium-stabilized zirconia, the substrate with the lowest thermal conductivity. For the other substrates, the dendritic instability could be generated only after introducing an artificial defect at the edge, enhancing the local induction. We find that the upper temperature threshold for the appearance of dendrites depends on the thermal conductivity of the substrate.

**Keywords** High temperature superconductors (HTS) · Dendritic flux instability · Thermal conductivity · Ultra-fast magneto-optical (MO) imaging

## 1 Introduction

Dendritic flux avalanches have been observed in several low- and high-$T_c$ superconductors, including $MgB_2$ [1–3], $Nb_3Sn$ [5], Nb [5], NbN [6], and $YBa_2Cu_3O_{7-x}$ (YBCO) [7–9], utilizing magneto-optical imaging (MOI) techniques [10]. The origin of these nonuniform flux patterns is thermomagnetic instability of the vortex matter in the superconducting films [11–16]. When vortices move through the material, energy is released, generating a local increase in temperature and this, in turn, decreases flux pinning, facilitating further flux motion. Such positive feedback may lead to thermal runaway and dramatic global flux redistribution.

While the dendritic flux structures tend to nucleate at preferred sites along the sample edges [17], they are irreproducible in detail, clearly showing the stochastic nature of the process. It has been predicted [11–16] that these flux avalanches will not develop unless some critical electric field, $E_c$, (or, equivalently, some critical magnetic-field sweep rate, $dB_a/dt$) has been exceeded. This threshold value depends on parameters such as the sample thickness, d, its critical current density, $j_c$, temperature, T, and the sample thermal conductivity, $\kappa$. The thermal conductivity plays an important role as it controls how fast any excess of heat, generated by flux motion, is dissipated from the area before the occurrence of instability. In the case of thin films, the substrate $\kappa$ and coefficient of heat transfer to the substrate are also important factors.

Reoccurring formation of dendritic flux patterns in YBCO films were previously observed only after locally heating the sample by a pulsed laser, triggering the instability at the location of the laser spot [7–9]. Exploiting our unique high speed MOI system [18], we have recently demonstrated that dendritic avalanches in YBCO films can be generated in the "conventional" way, namely,

---

E. Baruch-El (✉) · M. Baziljevich · Y. Yeshurun
Department of Physics, Institute of Superconductivity
and Institute of Nanotechnology and Advanced Materials,
Bar-Ilan University, 5290002 Ramat-Gan, Israel
e-mail: elranbe@gmail.com

M. Baziljevich · T. H. Johansen
Department of Physics, University of Oslo, 0316 Oslo, Norway

T. H. Johansen
Institute for Superconducting and Electronic Materials,
University of Wollongong, Northfields Avenue,
Wollongong, NSW 2522, Australia

by ramping up an external magnetic field [19]. The high speed MOI system enables real-time imaging at high rates (up to 68,000 fps), in addition to being capable of applying an external field at ultra-fast ramp rates (up to 3,000 T/s). Using the fast ramping capabilities of the system, and the field increasing effect from edge slits, we repeatedly generated dendrites in two different YBCO films. These results [19] were an important step towards establishing that dendritic flux instabilities are indeed a generic phenomenon in all type-II superconductors, including high-$T_c$ superconductors (HTS).

In this paper, we extend our investigation to explore the effect of the substrate thermal conductivity on the formation of dendrites in thin superconducting YBCO films grown on four different substrates.

## 2 Experimental

YBCO films with a thickness of 150 nm were produced by thermal reactive co-evaporation [20] on substrates made of $\alpha$-$Al_2O_3$ (sapphire), $SrTiO_3$ (STO), yttrium stabilized zirconia (YSZ), and magnesia (MgO). To ensure proper growth conditions, a 10 nm thick pre-coat of $CeO_2$ was used as a buffer layer on the first three substrates. There was no need for such a buffer layer on the MgO. The films had a transition temperature of $T_c = 87$ K and a critical current density of $j_c = 3.8$ MA/cm$^2$ at 77 K, when measured inductively. They were epitaxially grown, with the *c*-axis perpendicular to the surface. The substrates were cut into $4 \times 4$ mm$^2$ samples, suitable for magneto-optical (MO) imaging. In several of the samples, we cut a slit, 0.5–1 mm long and $\sim 80\,\mu$m wide, perpendicular to the film edges, using a wire saw. The introduction of slits were motivated by earlier theoretical works showing that planar defects enhances the external magnetic field locally; this increases the effective ramping rate and may facilitate thermal instability [21–23]. To make sure the samples were of sufficient quality, they were all checked both optically and magneto-optically before and after the cuts were made.

## 3 Results

MO imaging was performed after the samples were zero-field-cooled to 7 K and then exposed to an increasing perpendicular external field. Moderate sweep rates, typically in the order of 1 mT/s, were used in these initial tests. An overall smooth penetration front and Bean-like flux distribution were observed in all tests, confirming the high quality of the films. No avalanches were observed using these moderate sweep rates.

The investigation continued with the application of high field ramping rates. After zero-field cooling the samples to 7 K, the external field was ramped from 0 to 60 mT during 20 μs, and then, MO images were recorded. In the films grown on sapphire, STO, and MgO, this procedure did not produce any flux avalanches. Only after introducing a slit cut from the edge the fast ramping could trigger the instability, producing dendritic flux patterns. Figure 1a, b shows such images of YBCO grown on STO and sapphire, respectively. The dendritic flux structures originated from the cut at the right side of the films.

The results for the YBCO film grown on MgO were more diverse, as this sample appeared to be more stable. Using the same conditions as in the former measurements, the sample produced an avalanche only in a few rare cases. An example of such a dendritic pattern is shown in Fig. 2a. In order to routinely generate thermomagnetic instability in this sample, it was cooled to 7 K in the presence of a constant external field of −60 mT. The field was then removed and a reverse field of 60 mT applied with a ramping rate of 3 kT/s. This produced an extensive dendritic flux pattern, see Fig. 2b. The outline of the pattern is particularly clear as the invading flux meets anti-flux, producing a sharp zero-field border between the opposite field directions due to flux annihilation.

The YBCO film which had the most fascinating flux distributions was the one grown on YSZ. In this sample, avalanches were triggered even without the help of artificial edge cuts. A number of dendritic flux structures are visible in Fig. 3a, where an image was taken after increasing the

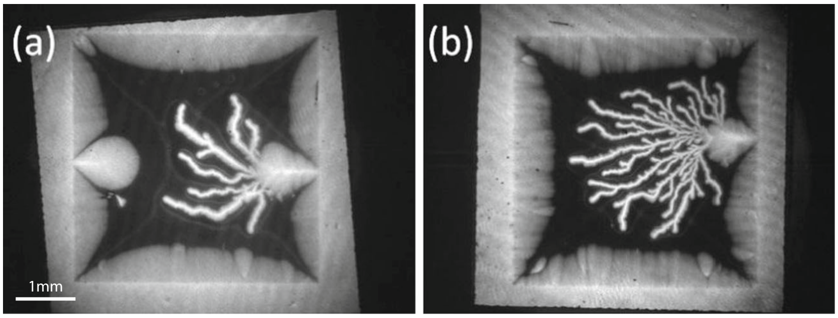

**Fig. 1** Magneto-optical images of YBCO samples grown on **a** STO and **b** sapphire, measured at T=7 K after a fast field ramp from 0 to 60 mT at a rate of 3 kT/s

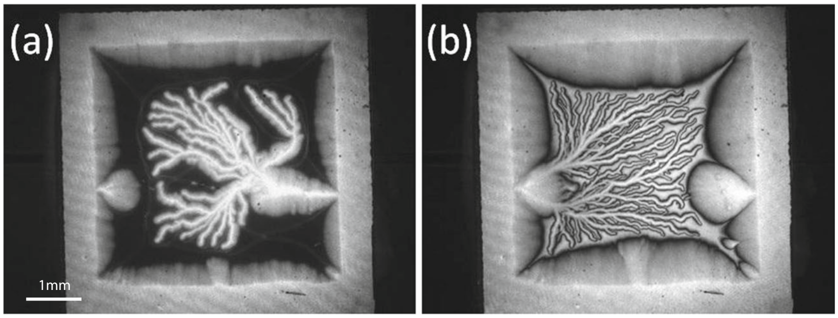

**Fig. 2** MO images of the YBCO film grown on MgO at 7 K. Cut defects have been deliberately introduced on both sides of the sample. **a** A rare case of dendritic flux penetration in a zero-field-cooled sample, using an applied field of 60 mT and a ramping rate of 3 kT/s. **b** Image taken after field cooling the film to 7 K in a −60 mT field and then exposing it to a 60 mT reverse field using a ramping rate of 3 kT/s

external magnetic field from 0 to 60 mT at a ramp rate of 3 kT/s. The sample temperature was 7 K. Later, a slit was cut from the right side of the sample to investigate its effect on the stability of the film. As can be seen in Fig. 3b, the penetrating flux configuration and overall dendritic morphology remain similar to those observed in the previous experiment, except that some of the branches now originate from the slit.

Another set of measurements was carried out to determine the upper threshold temperature [1, 2, 12] for the instability for the various YBCO/substrate combinations. In each case, a sample was zero-field-cooled to different target temperatures before the applied field was increased to 60 mT using the fastest ramping rate (3 kT/s). It was found that no avalanches were triggered above 59 K in the YBCO film grown on YSZ, defining its instability limit at this specific ramping rate. The corresponding threshold temperature for the films grown on sapphire or MgO was 40 K. In the case of the film grown on STO, dendrites were also observed up to 40 K. However, in this particular sample, we could not continue the experiments at higher temperatures as the flux avalanches caused permanent damage to the film.

## 4 Discussion

Except for being deposited on four different substrates, the YBCO films in this study were all produced by the same method and in the same deposition process [20]. Yet, the various YBCO/substrate combinations showed quite different results, demonstrating the major influence of the substrate on the thermomagnetic stability of the film. As suggested by theoretical models [12, 16], the key parameter in generating flux instabilities is the ratio of the magnetic and thermal diffusion, $t_m \backslash t_h = \tau = \mu_0 \kappa \sigma / C$, where $\sigma$ and C are the differential electrical conductivity and the specific heat, respectively, and $\kappa$ the thermal conductivity of the superconductor. A smaller $\tau$ favors flux avalanches. Though the expression for $\tau$ does not take into account heat transport into the substrate, it would be reasonable to assume that the substrate thermal conductivity, $\kappa_s$, should play an important role in modifying the effective $\tau$ of the various films we have investigated. From the literature, it can be established that the thermal conductivity of the different substrates differ significantly at 7 K; $\kappa_s \approx 0.05$, 4.5, 300, and 400–800 W/mK for YSZ [24], STO [25], MgO [26, 27],

**Fig. 3** Magneto-optical images of YBCO film on YSZ substrate at 7 K, using an external field of 60 mT and a ramping rate of 3 kT/s **a** without any artificially made defects and **b** with a slit cut into the upper right side of the sample

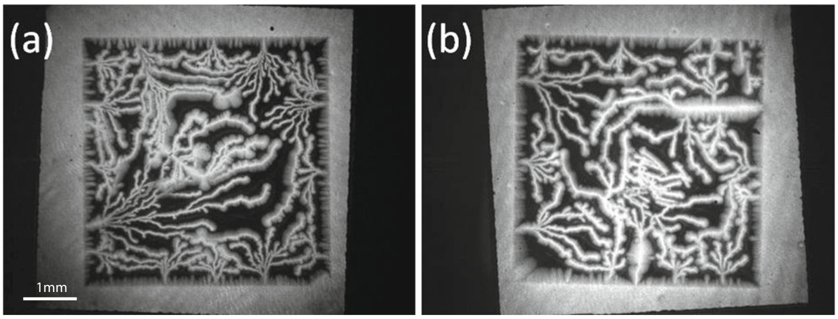

and sapphire [26, 27], respectively.

The YBCO films grown on YSZ, the substrate with the lowest $\kappa_s$, are by far the most unstable, generating a number of dendritic structures from multiple sources without a need to add artificial defects. As demonstrated above, STO, with larger $\kappa_s$, is indeed significantly more stable, and MgO, with $\kappa_s$ larger than that for STO, is even more robust against flux instabilities. In the MgO film, it was difficult to trigger flux avalanches even after a slit was cut into the sample edge. Surprisingly, sapphire, with the highest $\kappa_s$, is more unstable than MgO. This, we believe, is caused by the low thermal conductivity of the $CeO_2$ buffer layer that was deposited on the sapphire, but not on MgO. This buffer layer represents an additional obstacle to smooth thermal diffusion, decreasing the effective $\tau$ of the YBCO/sapphire film.

**Acknowledgments** The authors thank Dr. Robert Semerad for preparing samples and helpful discussions. We acknowledge a partial financial support from the Israel Science Foundation (Grant No. 164/12) and the Norwegian Research Council.

## References

1. Johansen, T.H. et al.: Europhys. Lett. **59**, 599 (2002)
2. Bobyl, A.V. et al.: Appl. Phys. Lett. **80**, 4588 (2002)
3. Albrecht, J. et al.: Appl. Phys. Lett. **87**, 182501 (2005)
4. Rudnev, I.A. et al.: Cryogenics **43**, 663 (2003)
5. Duran, C.A. et al.: Phys. Rev. B. **52**, 75 (1995)
6. Rudnev, I.A. et al.: Appl. Phys. Lett. **87**, 042502 (2005)
7. Leiderer, P. et al.: Phys. Rev. Lett. **71**, 2646 (1993)
8. Bujok, V. et al.: Appl. Phys. Lett. **63**, 412 (1993)
9. Bolz, U. et al.: Europhys. Lett. **64**, 517 (2003)
10. Magneto-Optical Imaging. In: Johansen, T.H., Shantsev, D.V. (eds.): NATO Science Series II, vol. 142. Kluwer Academic, The Netherlands (2004)
11. Mints, R.G., Rakhmanov, A.L.: Rev. Mods. Phys. **53**, 551 (1981)
12. Denisov, D.V. et al.: Phys. Rev. Lett. **97**, 077022 (2006)
13. Vestgarden, J.I. et al.: Phys. Rev. B **84**, 054537 (2011)
14. Vestgarden, J.I. et al.: Supercond. Sci. Technol. **26**, 055012 (2013)
15. Baziljevich, M. et al.: Physica C **369**, 93 (2002)
16. Dvash, E.E., Shapiro, I., Shapiro, B.Ya.: Phys. Rev. B **80** (2009)
17. Johansen, T.H. et al.: Surf. Sci. **601**, 5712 (2007)
18. Baziljevich, M. et al.: Rev. Sci. Instrum. **83**, 083707 (2012)
19. Baziljevich, M. et al.: Appl. Phys. Lett. **105**, 012602 (2014)
20. Utz, B. et al.: IEEE Trans. Appl. Supercond. **7**, 1272 (1997)
21. Mints, R.G., Brandt, E.H.: Phys. Rev. B **54**, 12421 (1996)
22. Gurevich, A.: Appl. Phys. Lett. **78**, 1891 (2001)
23. Gurevich, A., Friesen, M.: Phys. Rev. B **62**, 4004 (2000)
24. Yang, H.S. et al.: Acta Mater. **50**, 2309 (2002)
25. Suemune, Y.: J. Phys. Soc. Jpn. **20**, 174 (1965)
26. Kaiser, T.: PhD Thesis, University of Wuppertal (1998)
27. Slack, G.A.: Phys. Rev. Lett. **126**, 427 (1962)